A Hierarchical Multigrid Method for Oil Production Optimization

Hørsholt, Steen; Nick, Hamid; Jørgensen, John Bagterp

Published in:
IFAC-PapersOnLine

Link to article, DOI:
10.1016/j.ifacol.2019.06.110

Publication date:
2019

Document Version
Publisher's PDF, also known as Version of record

Available online at www.sciencedirect.com

ScienceDirect

IFAC PapersOnline CONFERENCE PAPER ARCHIVE

IFAC PapersOnLine 52-1 (2019) 492–497

A Hierarchical Multigrid Method for Oil Production Optimization

Steen Hørsholt * **Hamid Nick** ** **John Bagterp Jørgensen** *

* *Department of Applied Mathematics and Computer Science & Center for Energy Resources Engineering (CERE), Technical University of Denmark, DK-2800 Kgs. Lyngby, Denmark.*
** *Danish Hydrocarbon Research and Technology Centre, Technical University of Denmark, DK-2800 Kgs. Lyngby, Denmark*

Abstract: The large-scale optimization problems that arise from oil production optimization under geological uncertainty of industry-scale reservoir models poses a challenge even for modern computer architecture. In combination with ensemble-based methods for production optimization under uncertainty, gradient-based optimization algorithms provides a powerful approach that ensures a high convergence rate. However, the spatial resolution and complexity of typical industry-scale models has a significant computational impact that renders the optimization problem intractable. To reduce the computational burden model reduction is essential. In this paper, we introduce a grid coarsening method that maintains the overall dynamics of the flow, by preserving the geological features of the model. Furthermore, we present a hierarchical multigrid method for oil production optimization. The method utilizes a hierarchy of coarse level models based on the high-fidelity model. We present the workflow of the hierarchical multigrid optimization procedure and a numerical example that demonstrates the application of oil production optimization on a synthetic reservoir.

Keywords: Production optimization, Model reduction, Reservoir management, Work-flow, Gradient based optimization

1. INTRODUCTION

The increasing level of detail and complexity of reservoir models is a result of the modern reservoir characterization methods and geological modelling techniques. Together with a growing amount of data, this allows geologist to build high-resolution reservoir models able to reflect the geological heterogeneity. Geological reservoir models comprise detailed heterogeneous geological information at multiple length scales. Geological models is often at the resolution of 10^7 to 10^8 grid cells. Even with the computational capabilities of modern computers, the computational burden of such models is in many cases intractable. Therefore, model reduction (grid coarsening and property upscaling) is required to build reservoir models at a scale manageable for simulation. Upscaling techniques that are able to capture the heterogeneity effects of a high-resolution model has been a long-time focus of the research community (Christie, 1996; King and Mansfield, 1997; Durlofsky, 2005). The methods includes statistical averaging techniques and flow-based methods. The typical resolution of upscaled models is roughly, 10^5 to 10^6 cells, with simulation runtimes on the scale of hours. Production optimization workflows require a potentially very high number of reservoir simulations. In many cases, the direct use of high-fidelity models (upscaled geological model), will render the optimization problem computationally intractable. The computational load of the optimal control problem in a deterministic production optimization procedure depends on the size of the simulation model, the number of controlled wells and the number of control intervals. Different reduced-order modeling methods that provides for approximate but nonetheless fairly accurate simulation of models, has been proposed by van Doren et al. (2005) and by Cardoso and Durlofsky (2010). Oliveira and Reynolds (2015) propose the use of a hierarchical multiscale method for coarsening the control interval parametrization, based on control value and gradient criteria. Aliyev and Durlofsky (2015) proposes a multilevel procedure for optimizing well-placement and well-controls, which utilizes a gradient-free particle-swarm optimization algorithm. Krogstad et al. (2016) use a global upscaling procedure to compute a coarse model tuned to specific flow scenarios and applies an adjoint gradient-based optimization procedure.

In this paper, we introduce a model reduction procedure that reduces the computational impact of a high-fidelity model. The model reduction procedure consists of a coarsening procedure and an upscaling procedure and aims to reduce the turnover time compared to typical model reduction workflows. The coarsening method preserves geological features important for capturing the flow dynamics of the high-resolution model. To ensure flexibility in the choice of reservoir simulators we only consider logically indexed grids, i.e. corner-point grids. For the permeability upscaling, we apply a local single-phase flow-

⋆ The research leading to these results has received funding from the Danish Hydrocarbon Research and Technology Centre under the Advanced Water Flooding program.

10.1016/j.ifacol.2019.06.110

based procedure. We apply the approximate coarse-scale well model, proposed by Chen and Wu (2008) to upscale the well-index of well-bore completions. By applying these methods, we can significantly reduce the simulation time, while capturing the overall flow dynamics of the high-fidelity model. We introduce a hierarchical multigrid optimization procedure that optimizes an objective function over a multigrid hierarchy of coarsened-upscaled levels of a high-fidelity model. The procedure is presented from an oil industry perspective in Hørsholt et al. (2018b). The hierarchical multigrid optimization procedure integrates with our in-house gradient-based constrained optimization software tool RESOPT (Hørsholt et al., 2018a).

The structure of the paper is as follows. A short description of the dynamic optimization problem, including the system of differential algebraic equations that governs multi-phase flow in porous media, the net present value objection function and the optimal control problem. The next section describes the coarsening procedure, the grid property upscaling procedure and the well-index upscaling procedure. Next, we introduce the workflow of the hierarchical multigrid optimization procedure. Finally, we present a numerical example that demonstrates the optimization workflow in a deterministic water-flooding scenario. The example is a rate-controlled optimization of the well-known Egg-model (Jansen et al., 2013).

2. OPTIMAL CONTROL PROBLEM

In this section, we state the dynamic optimization problem and the underlying system of differential algebraic equations for multiphase flow in subsurface porous media, the net present value objective and the optimal control problem for oil production optimization.

2.1 Dynamic optimization problem

The dynamic optimization problem computes an open loop operating strategy that optimizes some performance measure over a given time horizon. We consider the dynamic optimization problem in the form

$$\min_{[x(t);y(t)]_{t_0}^{t_f},\{u_k\}_{k=0}^{N-1}} \varphi = \int_{t_0}^{t_f} \phi(y(t),u(t),\theta)\mathrm{d}t, \tag{1a}$$

subject to

$$x(t_0) = x_0, \tag{1b}$$
$$G(x(t),y(t),\theta) = 0, \quad t \in [t_0,t_f], \tag{1c}$$
$$\dot{x}(t) = F(y(t),u(t),\theta), t \in [t_0,t_f], \tag{1d}$$
$$u(t) = u_k \quad t \in [t_0,t_f], \ \ k = 0,\ldots,N-1, \tag{1e}$$
$$\{u_k\}_{k=0}^{N-1} \in \mathcal{U}. \tag{1f}$$

$x(t) \in \mathbb{R}^{n_x}$, is a vector of state varibles, $y(t) \in \mathbb{R}^{n_y}$, is a vector of algebraic variables, $u(t) \in \mathbb{R}^{n_u}$, is a vector of manipulated variables and, θ is a vector of geological parameters. $u(t)$ is discretized by a zero-order-hold parametrization defined by $u(t) = u_k, t_k \leq t \leq t_{k+1}, k = 0,\ldots,N-1$, where $t_N = t_f$ is the final time. The objective function, φ, in (1a) is some performance measure over the time horizon, $[t_0,t_f]$. Equations (1b)-(1e), constitutes the mathematical model of the dynamical process, which in this case is multiphase flow in porous media. Equation (1f) is the constraints on the manipulated variables.

Temporal discretization by the implicit Euler method gives the system of non-linear residual equations, $R_{k+1} = 0, k = 0,1,\ldots,N-1$. To allow for a more compact notation, we introduce the vectors, $\bar{x} = (x_1;x_2;\ldots;x_N,y_1;y_2;\ldots;y_N)$, $\bar{R} = (R_1;R_2;\ldots;R_N)$, and $\bar{u} = (u_0;u_1;\ldots;u_{N-1})$. In compact notation we write the residual equations as

$$\bar{R}\left(\bar{x},\bar{u},x_0;\theta\right) = 0. \tag{2}$$

2.2 Objective function and net present value

As a performance measure, φ in the dynamic optimization problem (1a), we consider the net present value. The net present value of an oil field is defined as a function, φ, of the states, $x(t)$, the algebraic variables, $y(t)$, the operating profile, $u(t)$, the initial state, x_0, and the geological parameters, θ. In continuous time the definition is

$$\varphi = \int_{t_0}^{t_f} \phi\left(t,x(t),y(t),u(t),\theta\right)\mathrm{d}t, \tag{3a}$$

where ϕ is the discounted profit rate

$$\begin{aligned}\phi &= \phi(t,x(t),y(t),u(t),\theta)\\ &= \mathrm{e}^{-d_c(t-t_0)/t_\tau} p(x(t),y(t),u(t),\theta),\end{aligned} \tag{3b}$$

and p is the profit rate

$$\begin{aligned}p = p(x(t),y(t),u(t),\theta) = \Big[& r_o q_{Os}(t) + r_g q_{Gs}(t)\\ & - \left(r_w q_{Ws}(t) + r_{w,\mathrm{inj}} q_{w,\mathrm{inj}}(t) + r_{g,\mathrm{inj}} q_{g,\mathrm{inj}}(t)\right)\Big].\end{aligned} \tag{3c}$$

$x(t)$ and $y(t)$ are the solution to (2), $u(t)$ is the operating profile. d_c is the continuous-time discount rate and t_τ is the discounted time interval (i.e. the time interval at which compound interest are ascribed). r_o and r_g are the sales prices of oil and gas. r_w is the water production cost, $r_{w,\mathrm{inj}}$ and $r_{g,\mathrm{inj}}$ are the water and gas injection cost. The corresponding surface flow rates for oil, gas, water, water injection and gas injection are, $q_{Os}, q_{Gs}, q_{Ws}, q_{w,\mathrm{inj}}, q_{g,\mathrm{inj}}$.

We apply the implicit Euler method for temporal discretization. Hence the net present value function in discrete-time is

$$\Phi\left(\bar{x},\bar{u},x_0;\theta\right) = \sum_{k=0}^{N-1} J_k\left(x_{k+1},u_k;\theta\right), \tag{4}$$

where the discounted net present value, J_k, for the k'th time interval is given by

$$\begin{aligned}J_k = & \frac{\Delta t_k}{(1+d)^{t_{k+1}/t_\tau}}\Big[r_o q_{Os,k+1} +\\ & r_g q_{Gs,k+1} - \left(r_w q_{Ws,k+1} + r_{w,\mathrm{inj}} q_{w,\mathrm{inj},k+1}\right)\Big].\end{aligned} \tag{5}$$

Note that the relation between the discrete-time discount rate, d, and the continuous-time discount rate, d_c, is $d_c = \ln(1+d)$.

2.3 Optimal control problem

The discrete-time constrained optimal control problem for oil production optimization is given by (Capolei et al., 2012)

$$\max_{\bar{u}\in\mathcal{U}} \quad \psi = \psi\left(\bar{u};x_0,\theta\right), \tag{6}$$

where the objective function is

$$\psi\left(\bar{u};x_0,\theta\right)=\left\{\Phi\left(\bar{x},\bar{u},x_0;\theta\right):\bar{R}(\bar{x},\bar{u},x_0;\theta)=0\right\}. \quad (7)$$

In this work, we only consider linear input constraints. The constraints are bounds on controls, rate of movement constraints on controls to prevent 'large' jumps, and bounds on total injection rates in each time step. We write the constraints as

$$\begin{aligned}\mathcal{U}=&\{\bar{u}:\bar{u}_{\min}\leq\bar{u}\leq\bar{u}_{\max},\\&\Delta\bar{u}_{\min}\leq\Delta\bar{u}\leq\Delta\bar{u}_{\max},\,b_l\leq\bar{A}\bar{u}\leq b_u\}.\end{aligned} \quad (8)$$

2.4 Black-box simulator

The optimization workflow presented in this paper does not dependent on any specific formulation and/or solution method of the governing equations (1b)-(1e). Thus we treat the reservoir simulator as a black-box function, $\mathcal{S}(\bar{u};x_0,\theta)$. For a simulator to be an eligible candidate for gradient-based production optimization purposes, it must fulfill the following requirements. Given an initial state, x_0, an operating profile, $\bar{u}$, and a geological realization vector, θ, the simulator must at every time-step return the states, $\bar{x}$, the net present value, ψ, and the gradient of the net present value with respect to the controls, $\nabla_{\bar{u}}\psi$.

$$[\bar{x},\psi,\nabla_{\bar{u}}\psi]=\mathcal{S}(\bar{u};x_0,\theta). \quad (9)$$

3. MODEL REDUCTION PROCEDURE

In this section, we outline the workflow of the model reduction procedure. We describe a practical grid-coarsening method, which preserve the geological features of a high-resolution model to a satisfactory degree for optimization purposes. We apply simple averaging of additive properties, e.g. porosity and net to gross and local flow-based upscaling for the absolute permeability. To capture the effect of high-resolution heterogeneity in the near well region, we upscale the well-index by the "near-well arithmetic averaging" method proposed by Chen and Wu (2008).

3.1 Coarsening

In this work, we only consider logical grids with ijk-indexing, i.e. Cartesian grids and corner-point grids. This means that all grid cell has exactly 6-faces. The grid indexing is defined by the "normal reading order", i.e. the $i-$index runs first, followed by the $j-$index and last by the $k-$index. The product of grid cells in each direction is the total number of grid cells, N_c. Formally a grid consists of a set of ijk-indexed grid cells, $\{c_n\}_{n=1}^{N_c}, N_c=N_xN_yN_z$.

To construct a coarse grid based on a high-resolution grid, $\{c_n\}_{n=1}^{N_{\text{fine}}}$, we group the fine grid into a number of subsets and amalgamate them into coarse grid cells, $\{c_n\}_{n=1}^{N_{\text{coarse}}}, N_{\text{coarse}}=N_{x,\text{coarse}}N_{y,\text{coarse}}N_{z,\text{coarse}}$. An amalgamated coarse grid is represented by a partitioning vector, $p\in N_{\text{fine}}$, that maps all fine grid cells into a coarse grid cell, i.e. $p_i=j$, if the fine grid cell, c_i, belongs to coarse grid cell, c_j. Although this allows for grouping arbitrary selections of fine grid cells into a subset, we only allow amalgamation of neighboring cells in the fine grid. The restriction that all cells has 6-faces means the corner nodes consists of the outermost fine-grid cell corner nodes. We note that this procedure does not preserve the reservoir volume. However, for the purpose of production optimization, this is of less importance. A simple way of computing the partitioning is to divide the dimensions of a fine grid by a coarsening factor in each direction, (cf_x,cf_y,cf_z). The coarse grid dimensions are then computed by

$$\begin{aligned}&(N_{x,\text{coarse}},N_{y,\text{coarse}},N_{z,\text{coarse}})=\\&(\lceil N_{x,\text{fine}}/cf_x\rceil,\lceil N_{y,\text{fine}}/cf_y\rceil,\lceil N_{z,\text{fine}}/cf_z\rceil).\end{aligned} \quad (10)$$

When there is no important geological features to account for, e.g. faults, this is a very robust method. In the gridding process for a faulted reservoir the geologist/engineer typically tries to align the grid with the fault directions. In this case we identify the direction and the, $ijk-$index of the faults and amalgamate cells on each side of the faults. By applying these techniques, we construct coarse corner-point grids that preserve the geological features of a high-fidelity model to a degree that is satisfactory for optimization purposes.

3.2 Flow-based upscaling

After the construction of a coarse-grid, the problem of populating the grid cell with properties, e.g. net to gross, porosity and permeability remains. There exist numerous property upscaling methods. The methods also depends on the type of the upscaled property. These methods includes simple averaging of properties over the fine grid to more advanced methods, such as flow-based permeability upscaling. For high-level coarsening of multi-phase flow systems, upscaling the relative permeability functions is often required. However, we do not consider relative permeability upscaling in this paper. For a more detailed discussion of these methods, we refer the reader to Barker and Thibeau (1997), and Renard and De Marsily (1997).

In this paper, we only consider upscaling of the following grid properties: net to gross, porosity and absolute permeability. We apply arithmetic average upscaling of the porosity and net to gross properties. To upscale the absolute permeability we apply local single-phase flow-based method. To upscale the absolute permeability we apply local single-phase flow-based method. By emulating a laboratory setup, we compute each component in the permeability tensor separately. The setup applies a pressure drop in each axial direction and keeps all other boundaries sealed. In the $x-$direction we compute the upscaled permeability, K_x^* in a coarse-grid cell as

$$K_x^*=\frac{q_{x,out}L_x}{L_zL_y(P_{out}-P_{in})}, \quad (11)$$

where, $q_{x,\text{out}}$, is the flow through the boundary, L_x,L_y,L_z, are the cell dimensions, and P_{in},P_{out} are the pressures at the boundaries. The absolute permeability in the, y and $z-$direction is upscaled by the same method.

3.3 Well-index upscaling

We upscale the well-index, WI, to capture the effects of the high resolution heterogeneous permeability in the near-well regions. The upscaling is computed by applying the method "near-well arithmetic averaging" proposed by Chen and Wu (2008). The method applies arithmetic averaging of the effective permeabilities, K_{eff}, along the

well trajectory within a coarse cell. We denote the fine scale permeability and the fine scale volume along the well trajectory in a coarse cell as, K_{fine} and, V_{fine}, respectively. The effective permeability averaging in a given direction is then computed as

$$K_{\text{eff}} = \frac{\sum K_{\text{fine}} V_{\text{fine}}}{\sum V_{\text{fine}}}. \tag{12}$$

The coarse scale well-index for a vertical well is computed using the Peaceman model by inserting the effective permeabilities:

$$\text{WI}_{\text{coarse}} = \frac{2\pi\sqrt{K_{x,\text{eff}} K_{y,\text{eff}}}\Delta z}{\ln\left(r_o/r_w\right)}. \tag{13}$$

4. HIERARCHICAL MULTIGRID OPTIMIZATION WORKFLOW

The optimization workflow presented in this paper utilizes a hierarchy of coarse level models, based on the high-fidelity model. In the following, we refer to the high-fidelity model as the basecase and the increasingly coarse models as levels. The levels are numbered in reverse order, i.e. in a set of coarse models consisting of, n, levels the coarsest level is labeled, level-n. By applying the coarsening-upscaling procedure presented in the previous section, we compute a hierarchy of coarse level models consisting of, n-levels. The optimization procedure starts at level-n, which is optimized with an initial guess of the operating profile. The computed set of optimal controls is then used as the staring guess on level-$(n-1)$. This procedure is repeated for each subsequent level. The optimization procedure can be stopped at any level depending on the aim of the optimization, time limitations and the computational resources available. Figure 1 illustrates the concept of the hierarchical multigrid optimization workflow.

5. CASE STUDY

As a case study we consider the well-known Egg-model proposed by (Jansen et al., 2013). The Egg-model is a three-dimensional synthetic two-phase flow reservoir model designed as a benchmark test case for production optimization. The model consist of 101 realizations of the permeability field. In this paper, we consider the first realization only.

5.1 Egg-model

The physical reservoir dimensions of the reservoir are, $(480, 480, 28)$m. It is discretized on a Cartesian grid with $(N_x, N_y, N_z) = (60, 60, 7)$ cells of uniform size, $(\Delta x, \Delta y, \Delta z) = (8, 8, 4)$ m. The total of number of cells are 25.200, where 18553 are active. The porosity is uniform, $\phi = 0.2$, and the permeability field is highly channelized. The reservoir has eight water injection wells and four producer wells. All wells are vertical and are completed throughout all layers in the $z-$direction. For a detailed description of the model see (Jansen et al., 2013).

5.2 Optimization parameters

The reservoir production is simulated for 3600 days with 120 control time-steps of length, $\Delta t = 30$ days. The water injection rate in all injector wells are subject to control, giving 960 controls, $\bar{u}$. The bottom-hole pressures in the producers are constant at 395 bar in all controls steps. All injection rates are bounded in the interval [0, 80] m^3/day and constrained by a rate of movement of 5 m^3/day between control intervals. The discount rate, d in (5) is set to 10%. The optimization is initialized with a water injection rate of, 79.0 m^3/day.

Table 1. Egg-model; optimization parameters.

Description	symbol	value	Metric
optimization strategy	deterministic	-	-
number of control steps	N	120	-
length of control steps	Δt	30	[day]
controls, water inj rates	q_{wi}	-	[m^3/day]
bound constraints	$q_{wi,\min}$	0.2	[m^3/day]
	$q_{wi,\max}$	80.0	[m^3/day]
rate of movement	rom	± 5	[m^3/day]
initial controls	u_{init}	79.0	[m^3/day]
prices	r_α	-	[US\$/m^3]
	r_o	283.04	[USD/m^3]
	r_w	37.74	[USD/m^3]
	r_{wi}	12.58	[USD/m^3]
discount factor	d	10%	-
optimization algorithm	SQP, interior-point	-	-
optimality tolerance	tol_{opt}	1e-6	-
step-size tolerance	tol_x	1e-6	-

Table 2. Egg-model grid coarsening levels.

Level	coarsening factor	grid dimensions	# cells	active cells
base-case	-	$(60, 60, 7)$	25200	18553
level-1	$(2, 2, 1)$	$(30, 30, 7)$	6300	4736
level-2	$(4, 4, 1)$	$(15, 15, 7)$	1575	1198
level-3	$(8, 8, 1)$	$(8, 8, 7)$	448	344

5.3 Model hierarchy

The multigrid hierarchy set consists of four levels of the Egg-model. For the model reduction procedure we keep the vertical resolution of the high-resolution model intact and apply three levels of coarsening factors, $(2, 2, 1), (4, 4, 1)$, and $(8, 8, 1)$. As mentioned earlier this does not preserve the grid volume, but this is not essential for the purpose of the optimization. Table 2 shows the details of the model reduction procedure. The base-case model properties are upscaled as described in section 3. The uniform porosity requires no upscaling. The absolute permeability is upscaled by the local flow-based method. The well-index is upscaled by the near well arithmetic averaging method. Figure 2 shows the Egg-model multigrid hierarchy with the upscaled horizontal permeability.

5.4 Optimization procedure

The hierarchical multigrid optimization procedure starts at level-3 (the coarsest level), where the optimization is initiated with, $\bar{u}_{\text{init}}$. After convergence the optimal controls, $\bar{u}^*_{\text{opt,level-3}}$, is passed on to the next level where it is used as the initial guess on the operating profile. This procedure continues through the hierarchy to the base-level. This gives us four sets of optimal controls denoted, $\bar{u}^*_{\text{opt,level-3}}, \bar{u}_{\text{opt,level-2}}, \bar{u}_{\text{opt,level-1}}, \bar{u}_{\text{opt,base-level}}$. At all levels in the hierarchy, we optimize by first applying a SQP-algorithm for a limited number of iterations and then

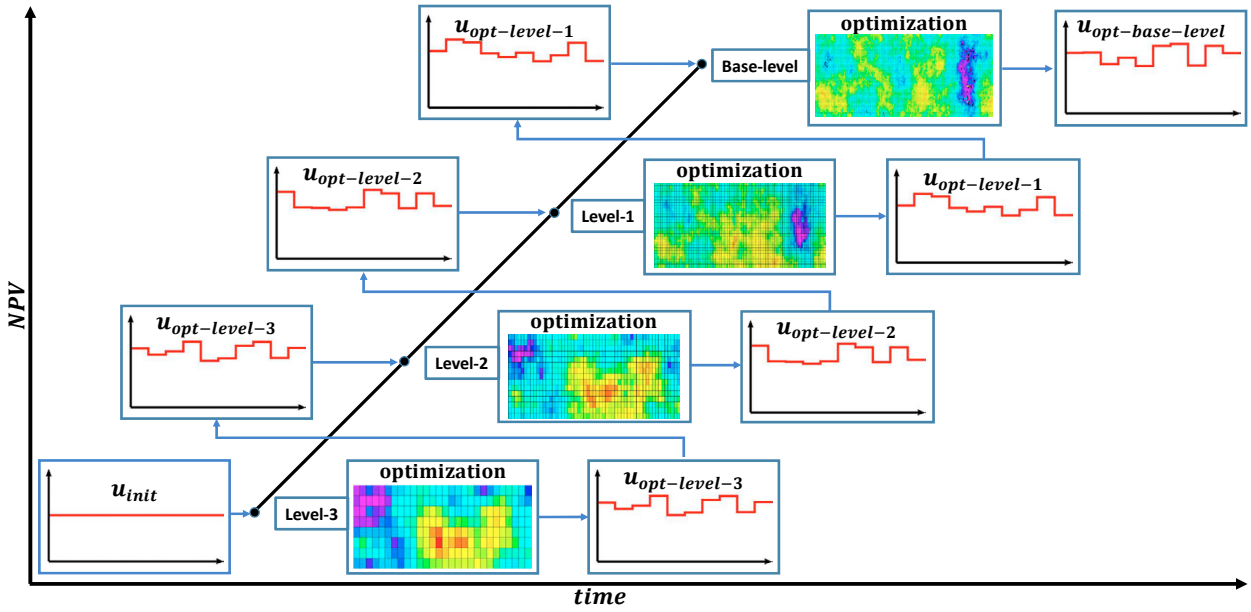

Fig. 1. Illustration of the hierarchical multigrid optimization workflow.

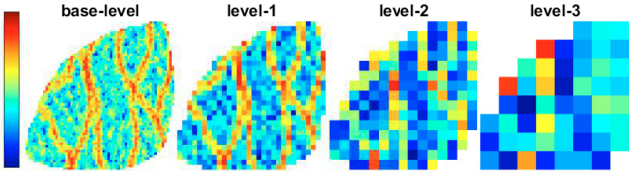

Fig. 2. Egg-model multigrid hierarchy.

Table 3. Combined SQP and interior-point strategy tolerances.

	SQP		interior-point	
level	max it	max sim	max it	max sim
level-3*	50	300	100	300
level-2	25	300	100	300
level-1	10	300	50	300
base-level	10	300	25	300
level-2*	50	300	100	300
level-1*	50	300	50	300
base-level	50	300	50	300

switching to an interior-point algorithm until convergence. We define the limit of the number of iterations and simulations for the two algorithms depending on the hierarchy level (see Table 3). For comparison reasons, we optimize all levels individually using the initial controls, $\bar{u}_{\text{init}}$, to get the optimal controls, $\bar{u}^*_{\text{opt,level-2}}, \bar{u}^*_{\text{opt,level-1}}, \bar{u}^*_{\text{opt,base-level}}$. All sets of optimal controls are evaluated by simulation at the base-level in the E100 simulator (Eclipse, 2016) and is compared to a reactive-strategy simulation. In the reactive-strategy case, a production well is shut-in if it becomes uneconomical, i.e. the water-cut rises above 0.88. All results obtained using the set of initial controls, $\bar{u}_{\text{init}}$, are marked with an superscript asterisk, *.

5.5 Results

Table 4 list the combined average forward simulation time and adjoint simulation time for all levels in the hierarchy. The table shows that there is a significant reduction in the simulation time for all lower levels in the hierarchy. However, as the reduction is directly dependent on the reduction in the number of grid cells the difference between levels decreases the lower the levels are. This means that one needs to consider the number of levels needed in the hierarchy. Table 5 list the results for all levels including the individual optimizations with initial controls, $\bar{u}_{\text{init}}$. Figure 3 shows iteration versus net present value. For the hierarchical multigrid optimization procedure, we see clear jumps in the objective value when moving from one level to the next. This is partially an effect of the fact that the coarsening/upscaling procedure does not preserve volumes. Furthermore, the coarser a level is, the worse the ability to capture of the flow dynamic of the high-fidelity model becomes. However, this is expected and not significant as long as we experience an increasing objective value, when evaluated at the high-fidelity level.

Table 4. Combined average simulation time for all levels in the hierarchy.

Hierarchy level	base-level	level-1	level-2	level-3
Simulation time [s]	210.24	31.94	15.69	113.14

Table 5. Hierarchical multigrid optimization results.

level	# iter	# sims	time [hour]	flag	NPV	E100
level-3*	46	351	2.079	max sim	89.7	81.7
level-2	27	261	1.313	$\Delta\bar{u}$	91.1	84.9
level-1	38	138	1.131	max it	88.0	89.5
base-level	19	193	8.592	max it	89.2	90.4
level-2*	66	318	1.644	$\Delta\bar{u}$	91.2	84.8
level-1*	67	370	3.532	max sim	86.7	87.8
base-level*	38	248	11.527	$\Delta\bar{u}$	88.7	89.9
Reactive-strategy						84.5

Evaluation of the obtained optimal controls at the E100-baselevel, shows that the net present value increases at every level. This is also the case for the individual level optimizations using, $\bar{u}_{\text{init}}$, as initial controls. Only optimization at the coarsest level, level-3*, is not able to

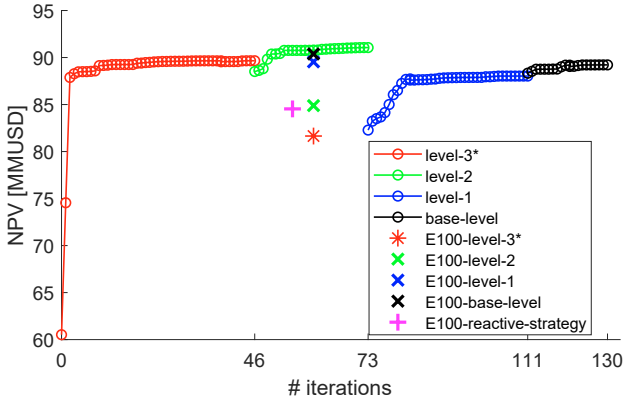

Fig. 3. Hierarchical multigrid optimization of all levels, and net present value evaluated in E100.

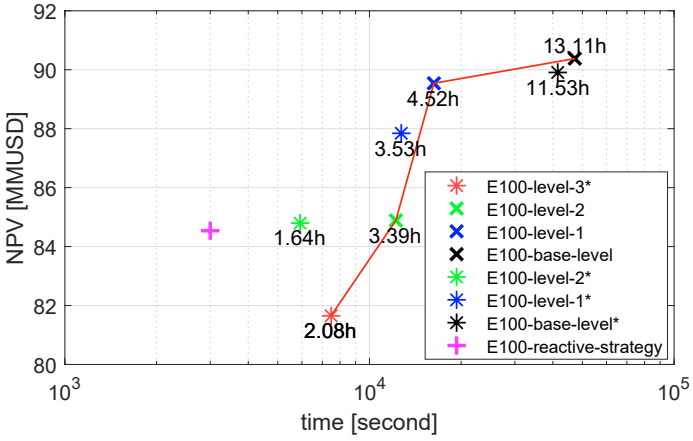

Fig. 4. Optimization of the Egg-model, computation time versus net present value evaluated in E100.

provide a net present value higher than that obtained by the reactive-strategy case.

Figure 4 shows elapsed time versus net present value for all level optimizations. At all levels, the hierarchical approach provides a higher net present value than the individual optimization runs at the corresponding level. The shape of curve is close to the ideal as depicted in the conceptual illustration in Figure 1. We partially credit this to the relatively simple two-phase fluid model, for which the single-phase flow-based upscaling method is well suited.

6. CONCLUSION

We have introduced a model reduction method for oil production optimization, which significantly decrease the computational impact of the forward simulations while maintaining the overall flow dynamics of the high-fidelity model. Furthermore, we introduce a hierarchical multigrid optimization procedure based on the model reduction method. The optimization procedure utilizes a hierarchy of coarsened and upscaled model levels based on a high-fidelity model. We demonstrate the model reduction method and the hierarchical multigrid optimization procedure workflow on the Egg-model (Jansen et al., 2013). The result shows a significant reduction of both the simulation run time and the number of performed optimization iterations.

REFERENCES

Aliyev, E. and Durlofsky, L.J. (2015). Multilevel field-development optimization using a sequence of upscaled models. In *SPE Reservoir Simulation Symposium*. Society of Petroleum Engineers.

Barker, J.W. and Thibeau, S. (1997). A critical review of the use of pseudorelative permeabilities for upscaling. *SPE Reservoir Engineering*, 12(2), 138–143.

Capolei, A., Völcker, C., Frydendall, J., and Jørgensen, J.B. (2012). Oil reservoir production optimization using single shooting and ESDIRK methods. *IFAC Proceedings Volumes*, 45(8), 286–291.

Cardoso, M.A. and Durlofsky, L.J. (2010). Linearized reduced-order models for subsurface flow simulation. *Journal of Computational Physics*, 229(3), 681–700.

Chen, Y. and Wu, X.H. (2008). Upscaled modeling of well singularity for simulating flow in heterogeneous formations. *Computational Geosciences*, 12(1), 29–45.

Christie, M.A. (1996). Upscaling for reservoir simulation. *Journal of Petroleum Technology*, 48(11), 1–004.

Durlofsky, L.J. (2005). Upscaling and gridding of fine scale geological models for flow simulation. In *8th International Forum on Reservoir Simulation Iles Borromees, Stresa, Italy*, 20–24.

Eclipse, S. (2016). *Reference Manual 2016.1, Schlumberger Inf.*

Hørsholt, S., Nick, H.M., and Jørgensen, J.B. (2018a). Oil production optimization of black-oil models by integration of matlab and eclipse e300. In *3rd IFAC Workshop on Automatic Control in Offshore Oil and Gas Production*.

Hørsholt, S., Nick, H.M., and Jørgensen, J.B. (2018b). Software for industrial scale oil production optimization. In *ECMOR XVI 2018 16th European Conference on the Mathematics of Oil Recovery*.

Jansen, J.D., Fonseca, R.M., Kahrobaei, S., Siraj, M., Van Essen, G., and Van den Hof, P. (2013). The egg model. *Delft University of Technology, The Netherlands, Tech. Rep., Research note and data set. htt p://repository. tudelft. nl/view/ir/uuid: 1b85ee17-3e58-4fa4-be79-8328945a4491 and http://data. 3tu. nl/reposi tory/uuid: 916c86cd-3558-4672-829a-105c62985ab2(accessed 23 March 2015)*.

King, M.J. and Mansfield, M. (1997). Flow simulation of geologic models. In *SPE Annual Technical Conference and Exhibition Sigma*, 331–346. Society of Petroleum Engineers.

Krogstad, S., Raynaud, X., and Nilsen, H.M. (2016). Reservoir management optimization using well-specific upscaling and control switching. *Computational Geosciences*, 20(3), 695–706.

Oliveira, D.F. and Reynolds, A. (2015). Hierarchical multiscale methods for life-cycle-production optimization: A field case study. *SPE Reservoir Simulation Symposium*, 2(05), 0896–0907.

Renard, P. and De Marsily, G. (1997). Calculating equivalent permeability: a review. *Advances in water resources*, 20(5-6), 253–278.

van Doren, J.F.M., Markovinović, R., and Jansen, J.D. (2005). Reduced-order optimal control of water flooding using proper orthogonal decomposition. *Computational Geosciences*, 10(1), 137–158.